HHS Public Access

Author manuscript

Stem Cell Res. Author manuscript; available in PMC 2021 December 20.

Published in final edited form as:

Stem Cell Res. ; 47: 101877. doi:10.1016/j.scr.2020.101877.

Extracellular vesicles released by adipose tissue-derived mesenchymal stromal/stem cells from obese pigs fail to repair the injured kidney

Alfonso Eirin[a], **Christopher M. Ferguson**[a], **Xiang-Yang Zhu**[a], **Ishran M. Saadiq**[a], **Hui Tang**[a], **Amir Lerman**[b], **Lilach O. Lerman**[a,b,*]

[a]Divisions of Nephrology and Hypertension, Mayo Clinic, Rochester, MN, United States

[b]Cardiovascular Diseases, Mayo Clinic, Rochester, MN, United States

Abstract

Aims: Mesenchymal stromal/stem cell (MSC)-derived extracellular vesicles (EVs) shuttle select MSC contents and are endowed with an ability to repair ischemic tissues. We hypothesized that exposure to cardiovascular risk factors may alter the microRNA cargo of MSC-derived EVs, blunting their capacity to repair the post-stenotic kidney in pigs with metabolic syndrome (MetS) and renal artery stenosis (RAS).

Methods: Porcine MSCs were harvested from abdominal fat after 16wks of Lean- or MetS-diet, and their EVs isolated and characterized using microRNA-sequencing. Lean- and MetS-EV protective effects were assessed in-vitro in human umbilical endothelial cells (HUVECs). To compare their in-vivo efficacy to repair ischemic tissues, allogeneic-EVs were intrarenally delivered in pigs after 6wks of MetS + RAS, and 4wks later, single-kidney renal blood flow (RBF) and glomerular filtration rate (GFR) were studied in-vivo, and microvascular architecture and injury ex-vivo. Lean-, MetS-, and MetS + RAS-sham served as controls (n = 6 each).

Results: Ten microRNAs, capable of targeting several pro-angiogenic genes, were upregulated in MetS-EVs versus Lean-EVs. In vitro, MetS-EVs failed to increase tube number and length, and to boost HUVEC migration compared to Lean-EVs. Lean- and MetS-EVs were detected in the

*Corresponding author at: Division of Nephrology and Hypertension, Mayo Clinic, 200 First Street SW, Rochester, MN 55905, United States. Lerman.Lilach@Mayo.Edu (L.O. Lerman).

Author contributions

A.E.: conception and design, collection and/or assembly of data, data analysis and interpretation, manuscript writing, final approval of manuscript. C.M.F.; X.Z.; I.M.S.; H.T.; A.L: collection and/or assembly data, data analysis and interpretation, final approval of manuscript. L. O.L.: conception and design, data analysis and interpretation, manuscript writing, final approval of manuscript.

CRediT authorship contribution statement

Alfonso Eirin: Conceptualization, Methodology, Data curation, Investigation, Validation, Writing - original draft. **Christopher M. Ferguson:** Methodology, Data curation, Investigation, Validation, Writing - review & editing. **Xiang-Yang Zhu:** Methodology, Data curation, Investigation, Validation, Writing - review & editing. **Ishran M. Saadiq:** Methodology, Data curation, Investigation, Validation, Writing - review & editing. **Hui Tang:** Methodology, Data curation, Investigation, Validation, Writing - review & editing. **Amir Lerman:** Methodology, Data curation, Investigation, Validation, Writing - review & editing. **Lilach O. Lerman:** Conceptualization, Supervision, Methodology, Data curation, Investigation, Validation, Writing - review & editing.

Conflict of interest statement

The results presented in this paper have not been published previously in whole or part, except in abstract format.

Appendix A. Supplementary data

Supplementary data to this article can be found online at http://doi.org/10.1016/j.scr.2020.101877.

stenotic-kidney 4wks after injection in the vicinity of small vessels. RBF and GFR were lower in MetS + RAS versus MetS, and restored in MetS + RAS + Lean-EVs, but not in MetS + RAS + MetS-EVs. Furthermore, MetS-EVs failed to restore renal expression of angiogenic factors, improve microvascular density, or attenuate fibrosis.

Conclusions: MetS alters the microRNA cargo of MSC-derived EVs and impairs their functional potency, limiting the therapeutic efficacy of this endogenous cellular repair system.

Keywords

Metabolic syndrome; Renovascular disease; Stem cells; MicroRNA

1. Introduction

Mesenchymal stem/stromal cells (MSCs) are multipotent adult cells with self-renewal capability that can differentiate into several cell types, and can be isolated from a diverse range of tissues, including fat. Renovascular disease (RVD) entails atheromatous stenoses of one or both renal arteries, and is an important cause of secondary hypertension (Hansen et al., 2002), as well as progressive loss of renal function (Lerman and Textor, 2001), which few interventions can halt. Importantly, exogenous delivery of MSCs bestows promising renoprotective effects in experimental (Eirin et al., 2014; Eirin et al., 2012; Ebrahimi et al., 2013) and clinical RVD (Saad et al., 2017), which are in part mediated by release of membrane-derived extracellular vesicles (EVs) (Aghajani Nargesi et al., 2017; Nargesi et al., 2017). In line with this, we have shown that intra-renal delivery of MSC-derived EVs preserves renal structure and function in chronic experimental RVD (Eirin et al., 2018; Eirin et al., 2017). The beneficial effects of EVs are partly attributted to their ability to increase intra-renal expression of angiogenic factors and blunt microvascular disease, an important determinant of renal function beyond a stenotic lesion (Chade, 2013).

EVs contain an important cargo of small noncoding microRNAs that regulate gene expression post-transcriptionally by directing their target mRNAs for degradation or translational repression (Eirin et al., 2014; Eirin et al., 2017). microRNA expression patterns are commonly altered in patients with obesity and other cardiovascular risk factors, often clustered in the metabolic syndrome (MetS). We have previously shown that MetS alters the microRNA content of EVs derived from porcine adipose tissue MSCs, modulating the expression of genes implicated in the development of MetS and its complications (Meng et al., 2018). Furthermore, in vitro studies have shown that obesity reduces the pro-angiogenic potential of adipose tissue stem cell-derived EVs by impairing the cargo of miR-126 (Togliatto et al., 2016). However, whether MetS-induced changes in the microRNA content of MSC-derived EVs impair their reparative function in vivo remains unknown.

In the current study, we took advantage of a novel swine model of MetS and renal artery stenosis (RAS) that recapitulates the metabolic and ischemic components of human RVD, and is characterized by prominent loss of intra-renal microvessels (Eirin et al., 2018). We tested the hypothesis that MetS alters the microRNA cargo of MSC-derived EVs, blunting their capacity to preserve the microvasculature, and in turn function, in the post-stenotic kidney.

2. Materials and methods

All animal experiments were performed with the approval of the Institution Animal care and Use Committee. Adipose tissue-derived MSCs were harvested from female pigs after 16 weeks of Lean (regular pig chow) or MetS (Pawar et al., 2015) (high fat/high fructose, Purina Test Diet, Richmond, IN) diet (n = 6 each), and their EVs isolated and characterized using microRNA-sequencing. Lean- and MetS-EV protective effects were assessed in-vitro in human umbilical endothelial cells (HUVECs). To compare their in-vivo efficacy to repair ischemic tissues, allogeneic-EVs were labeled before intrarenal delivery in pigs after 6 weeks of coexisting MetS and RAS (MetS + RAS). Four weeks later, single-kidney renal hemodynamics and function were studied in-vivo, and microvascular architecture and injury ex-vivo. Lean-, MetS-, and MetS + RAS-sham served as controls (n = 6 each).

2.1. MSC and EV isolation, characterization, and culture

MSCs were isolated from 5 to 10 g of omental fat tissue and cultured with advanced MEM medium (Gibco/Invitrogen) supplemented with 5% platelet lysate (Mill Creek Life Sciences, LLC, Rochester, MN) in 37 °C/5% CO2 (Eirin et al., 2014; Eirin et al., 2012; Eirin et al., 2014; Ebrahimi et al., 2013). Cells were then kept in cell recovery medium in −80 °C and characterized based on the expression of common MSC markers (CD44, CD90, and CD105) (Eirin et al., 2012; Eirin et al., 2014) and by trans-differentiation into osteocytes, chondrocytes, and adipocytes, as previously described (Eirin et al., 2014; Eirin et al., 2012; Eirin et al., 2014; Ebrahimi et al., 2013).

EVs were isolated from supernatants of MSCs (10 × 10^6) by ultracentrifugation, as previously described (Eirin et al., 2014). EVs were centrifuged twice (2000*g* and 100,000*g* for 1 h at 4 °C, Beckman Coulter Optima L-90 K), washed in serum-free medium 199 containing HEPES 25 mM, and centrifuged one more time. Pellets were then suspended and protein content quantified (Bradford method, BioRad). Limulus testing was performed to rule out endotoxin contamination (Charles River Lab.). EVs were characterized based on the expression of EV (CD40, β1, CD9, and CD81), and MSC (MHC-class I and CD44) surface markers (Eirin et al., 2014; Meng et al., 2018; Eirin et al., 2016).

2.2. EV microRNA cargo

High throughput microRNA sequencing and functional analysis was performed in Lean- and MetS-MSC-derived EVs (n = 5 each), as previously described (Eirin et al., 2014). Data were analyzed using the CAP-miRSeq-vl.l workflow (Sun et al., 2014) to generate aligned BAMs and excel files with both raw and normalized mature microRNA expression counts. Differential expression analysis was performed with EdgeR2.6.2 (Dudakovic et al., 2014; Robinson et al., 2010) to identify microRNAs upregulated in MetS-EVs compared to Lean-EVs (fold change > 2.0 and $p \leq 0.05$). Five microRNAs were randomly selected for validation, and their expression in Lean-EVs and MetS-EVs measured by quantitative polymerase chain reaction (qPCR). Because Met + RAS kidneys exhibit considerable microvascular rarefaction (Eirin et al., 2018), to elucidate whether microRNAs upregulated in MetS-EVs modulate angiogenic signaling, we used TargetScan7.1 to screen target genes associated with vascular development and anti-angiogenic genes (MGI database, http://

www.informatics.jax.org). Search Tool for the Retrieval of Interacting Genes (STRING) version 9.1 (http://string-db.org/) was used to predict associations among proangiogenic genes targeted by microRNAs upregulated in MetS-EVs. To explore whether microRNAS upregulated in MetS-MSCs were also selectively packed in EVs, we performed microRNA sequencing in MetS-MSCs and their daughter EVs. MicroRNAs with fold change (EVs/MSCs) > 2.0 and $p \leq 0.05$ were considered enriched in EVs.

2.3. EV mRNA and protein cargo

The genetic and protein content of pro-inflammatory and anti-inflammatory factors of Lean- and MetS-MSC-derived EVs was assessed using mRNA sequencing and liquid chromatography mass spectrometry (LC-MS/MS) proteomic analysis as previously described (Eirin et al., 2014; Eirin et al., 2016). For mRNA sequencing, RNA libraries were prepared (TruSeq Prep Kit, Illumina) and cells sequenced on an Alumina HiSeq 2000 using TruSeq SBS and HCS data collection software. mRNA-seq data were analyzed using the MAPRSeq system and TopHat (Kalari et al., 2014; Kim et al., 2013) and gene Counts software (Liao et al., 2014). Normalization and differential expression analysis was performed using edgeR 2.6.2 (Robinson et al., 2010). For LC-MS/MS, EV pellets were solubilized and lysed, and protein samples denatured. Aliquots were resolubilized and samples electrophoresed in 4 ± 20% TGX Ready gels at 200 V for 30 min. Gel sections were digested with trypsin (Hogan et al., 2015), and peptides extracted and transferred onto a 35cmx100μm PicoFrit, self-packed with Agilent Poroshell 120S 2.7 μm EC-C18 stationary phase, using a Dionex UltiMate 3000 LC system (Thermo-Fisher). Peptides were separated and eluting peptides analyzed using a QExactive mass spectrometer and analyzed using label-free peptide MSI intensity-based methods. Data quality was assessed using MaxQuant 1.5.1 software (Cox et al., 2014) and protein group intensities of each sample log2 transformed, normalized, and modeled using a Gaussian-linked generalized linear model (Kim and van de Wiel, 2008). mRNAs and proteins with fold-change (MetS-EVs/Lean-EVs) > 1.4 and $p < 0.05$ (Lean-EVs vs. MetS-EVs) were classified as upregulated in MetS-EVs, whereas those with fold-change < 0.7 and $p < 0.05$ were considered downregulated in MetS-EVs. TargetScan7.1 was used to screen pro-inflammatory and anti-inflammatory genes (MGI database).

2.4. EV function

EV pro-angiogenic effects were assessed by their capacity to induce HUVECs (PromoCell, Heidelberg, Germany) to proliferate, migrate, and form tube-like networks on matrigel (Chade et al., 2009; Choi et al., 2004). These functional attributes were assessed in HUVECs incubated alone, or in combination with Lean-EVs or MetS-EVs. HUVEC migration was measured using a Boyden Chamber assay (Millipore 5 μm QCM Chemotaxis Cell Migration Assay, Millipore Sigma, Burlington, MA cat#: ECM506) (Chen et al., 2014). The Boyden Chamber system uses a hollow plastic chamber, sealed at one end with a porous membrane. Cells were placed inside the 24-well-colorimetric chamber and allowed to migrate through the pores to the other side of the membrane. Migratory cells were then stained by crystal violet and quantified by spectrophotometry at an optical density of 560 nm (SynergyMx, BioTek Instruments Inc., Winooski, VT).

HUVEC proliferation was assessed in real time using IncuCyte Zoom (Essen Biosciences Inc.) (Miller et al., 2017; Moran-Jones et al., 2015). Cells were harvested in M199 media with 3% FBS and 2500 cells/well were seeded onto a 96-well tissue-culture plate. Cell growth was monitored by capturing phase contrast images every 2 h for 120 h and analyzed using the integrated confluence algorithm.

Tube formation was assessed as previously described (Chade et al., 2009). Matrigel (BD Biosciences, Bedford, MA) was spread onto 24-well plates (Coster, Coming Inc., Corning, NY) and allowed to polymerize for 15 min at 37 °C. HUVECs (4x10^4) were plated on matrigel precoated well plates and incubated at 37 °C for 24 h with EGM-2 culture medium. Tube length and number were counted in 4 random (x20) fields per subject and measured using Image-J (Version 1.5, National institute of Health) (Schneider et al., 2012). Experiments were done in triplicate and observers blinded to cell type and group.

2.5. In vivo studies

To compare the in-vivo efficacy of Lean and MetS-MSCs to repair ischemic tissues, Lean- and MetS-MSCs were cultured to generate an allogeneic pool of Lean- and MetS-EVs, which were subsequently labeled with a red fluorescence dye (PKH26, Sigma) and injected into RAS kidneys.

Additional domestic female pigs started a 16-week MetS diet (n = 18). After 6 weeks of diet, animals were anesthetized with tile-tamine hydrochloride/zolazepam hydrochloride (0.25 g IM, Telazol®) and xylazine (0.5 g). Anesthesia was maintained with ketamine (0.2 mg/kg/min IV) and xylazine (0.03 mg/kg/min). Unilateral RAS was induced in these pigs by placing a local-irritant coil in the main renal artery using fluoroscopy (Lerman et al., 1999), whereas sham renal angiography was performed in Lean and MetS pigs.

Six weeks after induction of RAS, pigs were similarly anesthetized and the degree of stenosis determined using renal angiography. MetS + RAS pigs received a single infusion of 1 × 10^10 allogeneic Lean- or MetS-EVs (a dose commonly used for intrarenal delivery (Eirin et al., 2018; Eirin et al., 2017), or vehicle, into the stenotic kidney over 5 min through a 5F catheter positioned in the renal artery proximal to the stenosis (n = 6 each). Lean and MetS pigs underwent only sham procedures (angiography, saline infusion) and served as controls.

Four weeks later, systemic blood samples were collected for cholesterol fractions, fasting glucose and insulin levels, and insulin resistance, which was calculated by the homeostasis model assessment of insulin resistance (HOMA-IR) (Pawar et al., 2015). Single-kidney hemodynamics and function were determined using multi-detector computed tomography (MDCT). Under fluoroscopic guidance, catheters advanced into the stenotic and inferior renal cava (IVC). Blood pressure was monitored with an intra-arterial catheter during MDCT studies.

One or two days after completion of in vivo studies, pigs were euthanized with sodium pentobarbital (100 mg/kg IV, Sleepaway, Fort Dodge Inc.) (Eirin et al., 2014). Kidneys were harvested using a retroperitoneal incision, dissected, and sections frozen in liquid nitrogen

(and maintained at −80 °C) or preserved in formalin for histology and ex-vivo studies. A lobe of kidney tissue was perfused and prepared for micro-CT studies.

2.6. Renal function

Single-kidney volume, renal blood flow (RBF), and glomerular filtration rate (GFR) were measured by MDCT (Somatom Sensation-128, Siemens Medical Solution, Forchheim, Germany) scanning, as previously shown (Chade et al., 2009; Ferguson et al., 2018; Ferguson et al., 2019; Eirin et al., 2012; Zhu et al., 2004; Krier et al., 2001). After a central venous bolus of iopamidol (0.5 ml/kg over 2 s), 140 consecutive scans (330 ms each) were acquired. Cortical and medullary regions of interest (ROIs) were traced using Analyze™ (Biomedical Imaging Resource, Mayo Clinic, Rochester, MN). ROIs were then used to calculate single kidney regional perfusion using MATLAB 7.10 (MathWorks), whereas renal volume was calculated using planimetric methods. RBF was calculated by summing the product of cortical perfusion and volume and the product of medullary perfusion and volume. GFR was calculated from the cortical curve slope (Krier et al., 2001).

2.7. EV tracking

Labeled EVs were tracked and localized in frozen 5 μm sections of the stenotic kidneys by immunofluorescence staining with the endothelial marker CD31 (Abeam, cat# ab28364). The average number EVs/mm2 cross-section was multiplied by section thickness (5 μm) and kidney volume, and then divided by the number injected to yield retention rate (% of injected amount), as previously described (Eirin et al., 2018; Eirin et al., 2017).

2.8. Microvascular remodeling and angiogenesis

Renal microvascular architecture was assessed using micro-CT, as previously described (Eirin et al., 2012). Kidney segments were perfused (Microfil MV122) with a radio-opaque silicone polymer (Flow Tech, Carver, MA) using a saline-filled cannula ligated within a segmental artery. Samples were prepared and scanned, and images analyzed using Analyze™ to calculate spatial density of cortical microvessels and microvascular tortuosity (Zhu et al., 2004). In addition, renal tissue sections were stained with a-smooth muscle actin (SMA, DakoCytomation A/S, Glostrup, Denmark) and media-to-lumen ratio calculated. Renal expression of hepatocyte growth factor (HGF), vascular endothelial growth factor (VEGF), and VEGF receptor (VEGFR)-2, was assessed by Western Blotting.

2.9. Renal injury pathways

Tubular injury was assessed in 5-μm mid-hilar cross-sections of the kidney stained with periodic acid-Schiff (PAS) (Eirin et al., 2012). Tubular injury, including dilation, atrophy, cast formation, cell detachment, or thickening of tubular basement membrane, was scored from 1 to 5. We defined 0 as normal tubules, 1: < 10% of tubules injured, 2: 10–25%, 3: 26–50%, 4: 51–75%, and 5: > 75% of tubules injured. Tubulo-interstitial fibrosis was assessed in trichrome stained slides using a computer-aided image analysis program (ZEN® 2012 blue edition, Carl ZEISS). In each slide, trichrome staining was semi-automatically quantified in a blinded manner in 15–20 fields, expressed as fraction of kidney surface area, and the results from all fields averaged (Eirin et al., 2011; Chade et al., 2004).

2.10. Statistical methods

Statistical analysis was performed using JMP 14.0 (SAS Institute, Cary, NC, USA). Results were expressed as mean ± SD or median (interquartile range). Parametric (ANOVA/Student *t*-test) and non-parametric (Wilcoxon/Kruskal-Wallis) tests were used as appropriate, and significance accepted for $p \leq 0.05$.

3. Results

3.1. MetS alters the microRNA cargo of EVs

Next-generation sequencing analysis revealed 10 microRNAs upregulated in MetS-EVs compared to Lean-EVs (Fig. 1A). Expression of representative microRNAs by qPCR followed the same patterns as the sequencing findings. Specifically, miR-132, miR-145–3p, and miR-199a-5p were higher in MetS-EVs compared to their Lean counterparts, whereas miR-27b-3p, and miR-Let-7c did not differ between them (Fig. 1B).

3.2. microRNAs upregulated in MetS-EVs target pro-angiogenic genes

Target gene prediction analysis of microRNAs enriched in MetS-EVs indicated that they are capable of targeting over half (382 out of 749) of the genes associated with several aspects of vascular development (Fig. 2A), as well as (36 out of 164) anti-angiogenic genes (Fig. S1) (MGI, vasculature development, G0:0001944). Among their targets are genes involved in renal system and glomerulus vasculature development, and endothelial cell differentiation (Table S1). The microRNAs upregulated in MetS-EVs were also well linked, manifested in a total of 1498 known or predicted interactions between pro-angiogenic genes that they target. These included protein binding, signaling receptor binding, enzyme binding, and transcription factor binding interactions (Fig. 2B), as well as a number of genes involved in VEGF signaling.

3.3. MetS alters the inflammatory mRNA and protein cargo of EVs

Next-generation sequencing analysis revealed 40 pro-inflammatory genes upregulated and 15 anti-inflammatory genes downregulated in MetS-EVs compared to Lean-EVs (MGI, inflammatory response, G0:0006954) (Fig. S2A). Similarly, LC-MS/MS proteomic analysis identified 31 pro-inflammatory proteins upregulated and 10 anti-inflammatory proteins downregulated in MetS-EVs compared to Lean-EVs (Fig. S2B).

3.4. MetS-EVs fail to induce endothelial cell tube formation in vitro

HUVEC proliferation was similar among the groups (Fig. 3A, $p > 0.05$ ANOVA). Cell migration was augmented in HUVECs treated with both types of EVs, although this magnification was greater in HUVEC + Lean-EVs compared to HUVECs + MetS-EVs (Fig. 3B). The number and length of tube-like structures on Matrigel were again higher in HUVECs + Lean-EVs versus untreated HUVECs and HUVECs treated with MetS-EVs (Fig. 3C).

3.5. MetS-EVs fail to repair ischemic tissues in vivo

Table 1 summarized the systemic characteristics and renal function in all study groups at the end of the study. Body weight and blood pressure were similarly higher in MetS, MetS + RAS, MetS + RAS-Lean-EVs, and MetS + RAS-MetS-EVs compared to Lean. All RAS pigs exhibited moderate, but significant stenoses of a similar degree ($p > 0.05$ ANOVA). Total cholesterol, high-density lipoprotein (HDL), low-density lipoprotein (LDL), and triglyceride levels were comparably higher in all MetS groups versus Lean. Although fasting glucose levels did not differ among the groups, fasting insulin and HOMA-IR levels were higher in all MetS groups (Pawar et al., 2015). Single-kidney volume, RBF, and GFR were higher in all MetS compared to Lean, consistent with obesity-induced hyperfiltration. These parameters all decreased in MetS + RAS post-stenotic kidneys, but were restored to MetS levels only in MetS + RAS + Lean-EVs (Table 1).

3.6. EVs were retained in the stenotic kidney

MSC derived EV retention rate in the stenotic kidney 4 weeks after intra-arterial administration ranged between 2 and 3%, with no differences observed between Lean- and MetS-EVs. MSC-derived EVs were mainly detected in the tubulo-interstitium of the post-stenotic swine kidney four weeks after intra-renal administration (Fig. 4A). EV clusters were similarly identified in the vicinity of small vessels of Lean-EV and MetS-EV-treated kidneys (Fig. 4B).

3.7. MetS-EVs failed to improve renal microvascular remodeling in vivo

Spatial density of cortical microvessels that was diminished in MetS compared to Lean kidneys, and further reduced in MetS + RAS, improved in MetS + RAS pigs treated with Lean-EVs. Contrarily, no improvement was observed in MetS + RAS pigs treated with MetS-EVs (Fig. 5). Microvascular tortuosity, which indicates vessel immaturity, was higher in MetS compared to Lean and further increased in MetS + RAS, but normalized only in Lean-EV-treated pigs. Renal expression of the pro-angiogenic factor HGF was similarly lower in all treated or untreated MetS + RAS groups compared to Lean and MetS (Fig. 6A). On the other hand, expression of VEGF and VEGFR-2, which decreased in MetS + RAS compared to Lean and MetS, normalized only in MetS + RAS + Lean-EVs. Vessel wall-to-lumen ratio, which reflects microvascular remodeling, was higher in MetS compared to Lean kidneys, further increased in MetS + RAS, and decreased in MetS + RAS + Lean-EVs, but remained unchanged compared to MetS + RAS in MetS + RAS + MetS-EVs (Fig. 6B).

3.8. MetS-EVs did not attenuate renal fibrosis

Tubular injury score and tubulo-interstitial fibrosis were markedly higher in MetS + RAS compared to Lean and MetS, decreased in MetS + RAS + Lean-EVs, but not in MetS + RAS + MetS-EVs (Fig. 7).

4. Discussion

Our study demonstrates that MetS alters the cargo of porcine EVs isolated from adipose tissue-derived MSCs, leading to selective packaging of microRNAs capable of targeting

primarily pro-angiogenic genes. Transfection of HUVECs with MetS-EVs blunted the number and length of tubes that these cells form in the Matrigel assay, and produced a lesser increment in HUVEC migration versus Lean-EVs. Intra-renal delivery of Lean-EVs in pigs with MetS + RAS restored renal expression of angiogenic factors and improved microvascular density, medullary oxygenation, and renal function. Contrarily, these beneficial effects were abolished in animals treated with MetS-EVs. These findings suggest functional impairment in the endogenous cellular repair system in subjects with MetS, which might be related to their microRNA content and interfere with their capacity for self-repair. Furthermore, approaches to improve the therapeutic efficacy of autologous exogenous EVs isolated from adipose tissue-derived MSCs might be useful for patients with MetS.

MetS remains a growing world epidemic that affects over 20% of adults in western populations (Cameron et al., 2004). MetS is clinically characterized by the co-existence of cardiometabolic risk factors, including obesity, insulin resistance, hypertension, hyperglycemia or dyslipidemia, and significantly increases the risk of diabetes mellitus and cardiovascular disease and chronic kidney disease (Alberti et al., 2006; Roberts et al., 2013; Chen et al., 2004).

MSCs constitute an important element of the endogenous cellular repair system, and execute their reparative function via intercellular communication with target cells. Considerable experimental evidence shows that their beneficial effects are in part attributed to paracrine release of soluble mediators as well as membranous EVs (Aghajani Nargesi et al., 2017). In support this notion, we have shown that delivery of EVs isolated from adipose tissue-derived MSCs improved porcine stenotic kidney function and structure (Eirin et al., 2017). Porcine adipose tissue-derived MSCs have similar differentiation capacity, but exhibit higher growth rate and longer population doubling time in an inflammatory environment compared to porcine MSC lines obtained from different tissue origins, including fat, skin, and peripheral blood (Calle et al., 2018). Importantly, adipose tissue-derived MSC-derived EVs obtained from healthy pigs restored the expression of angiogenic factors and increased cortical microvascular density in pigs with RVD (Eirin et al., 2018); underscoring the potential of cell-free therapies to preserve the microcirculation and function of the kidney

As effectors of their parent cell intercellular communication system, EVs are enriched with a biologically active cargo of proteins and genes, which exert tissue trophic and reparative effects in recipient cells (Aghajani Nargesi et al., 2017; Nargesi et al., 2017). Furthermore, EVs transport gene regulatory information in the form of microRNAs, which play important roles in post-transcriptional regulation of biological processes by degradation or translational repression. For example, we have previously identified a significant number of interactions between mRNAs and microRNA targets enriched in EVs isolated from adipose tissue-derived MSCs, suggesting post-transcriptional control of cellular function in recipient cells (Eirin et al., 2017). Thus, the microRNA cargo component of EVs is an important determinant of their impact on the target cell.

Pertinently, the microRNA cargo of EVs is reflective of the state of the parent cell, which can be impacted by cardiovascular risk factors. A 16-week high fat/high fructose (MetS) diet

alters the expression of microRNAs in porcine adipose tissue MSCs (Pawar et al., 2019), and in turn interferes with the microRNA content of their daughter EVs, modulating the expression of genes implicated in the development of MetS and its complications (Meng et al., 2018). The current study extends our previous observations and shows that MetS also alters the microRNA cargo of EVs isolated from adipose tissue-derived MSCs that regulates angiogenic signaling. We identified 10 microRNAs upregulated in MetS-EVs compared to Lean-EVs. Notably, these microRNAs are capable of targeting over 50% of all genes related to vascular development, including promotion of angiogenesis in the glomerulus and renal system, as well as endothelial cell differentiation. Interestingly, we identified multiple interactions among those pro-angiogenic genes targeted by microRNAs upregulated in MetS-EVs, suggesting that these genes normally operate in concert to promote blood vessel development. Thus, their repression by microRNAs may affect a myriad of angiogenic signaling pathways.

microRNAs upregulated in MetS-EVs can also target a fraction of anti-angiogenic genes, including angiomotin (AMOT), which mediates the inhibitory effect of angiostatin on tube formation and migration of endothelial cells (Troyanovsky et al., 2001), and phosphoglycerate kinase-1, which encodes for a glycolytic enzyme that favors release of the blood vessel inhibitor angiostatin and reduces secretion of VEGF (Wang et al., 2007) and HGF (Wajih et al., 2003). However, these microRNAs target a significantly higher number of pro- than anti-angiogenic genes (51.0% vs. 21.9%), suggesting that MetS-EVs preferentially target and likely inhibit pro-angiogenic genes.

In line with this, our in-vitro studies showed that MetS-EVs failed to increase the number and length of tubes and produced a lesser augmentation in HUVEC migration compared to Lean-EVs. These results are in agreement with previous studies showing that stem cell-derived EVs from obese subjects have reduced content of miR-126, which impair their pro-angiogenic potential in vitro (Togliatto et al., 2016). Although we did not identify miR-126 enriched in MSC-derived EVs isolated from MetS pigs, possibly due to interspecies variability, our observations support the notion that the cargo of several microRNAs capable of targeting pro-angiogenic pathways might be in part responsible for the diminished reparative capacity of MetS-EVs.

We have also investigated the inflammatory cargo of EVs, and found that the content of pro-inflammatory genes and proteins was greater in MetS-EVs compared to their Lean counterparts, in line with our previous observations (Eirin et al., 2014; Eirin et al., 2012). Contrarily, expression of anti-inflammatory mRNAs and proteins was higher in Lean-EVs versus MetS-EVs, suggesting that MetS promotes selectively packaging of specific pro-inflammatory signatures that may impair the ability of EVs to repair damaged tissues.

To further test whether MetS-induced changes in EVs isolated from adipose tissue-derived MSCs interferes with their ability to repair the renal microcirculation in vivo, MetS + RAS pigs were treated with either Lean- or MetS-EVs. Four weeks after intra-renal delivery, EV clusters were detected in the tubulo-interstitium of porcine stenotic kidneys, with some in the vicinity of small vessels. We have previously shown that approximately 2% of injected EVs are selectively retained in the stenotic kidney by 4 weeks after intra-renal delivery

(Eirin et al., 2017). In this study, despite similar retention of Lean- and MetS-EVs, the vasculoprotective effect was abolished in animals treated with MetS-EVs. MetS-EVs failed to increase the number of cortical microvessels and improve microvascular remodeling, reflected in higher vessel tortuosity and media-to-lumen ratio. This might have been in part due to attenuated upregulation of renal expression of angiogenic factors, including VEGF (targeted by miR199a-5p and miR-145–3p) and VEGFR2 (targeted by miR-199a-3p), which are crucial for preserving the microvasculature in RVD (Chade, 2011). Importantly, MetS-EVs also failed to ameliorate tubular injury and fibrosis, which may partly explain the lack of improvement in renal hemodynamics and function. Therefore, MetS-induced changes in the microRNA cargo of EVs isolated from adipose tissue-derived MSCs may have limited their pro-angiogenic potential and their ability to bestow improvement in renal structure and function in MetS + RAS pigs.

We acknowledge limitations to our in-vivo study, including the use of relatively young female pigs and the short duration of MetS and RAS. Gender and age are important determinants of MetS that may also influence the reparative capacity of MSC-derived EVs. While gender does not seem to affect the paracrine function of MSCs (Siegel et al., 2013), young MSC-derived EVs manifest superior reparative potency compared to aging EVs (Huang et al., 2019), implying that age adversely impacts EV function. Our model displayed several characteristics related to human MetS, including obesity, hypertension, hyperlipidemia, and insulin resistance, which were associated with changes in the microRNA cargo of MSC-derived EVs. Furthermore, our MetS + RAS model closely mimics the coexistence of the ischemic and metabolic microenvironments of human RVD, leading to microvascular disease, tubular injury, fibrosis, and impaired renal function. To characterize their microRNA cargo, EVs were isolated using the ultracentrifugation method. However, further studies using size exclusion chromatography, which better preserves the biophysical properties of EVs (Reiner et al., 2017; Mol et al., 2017), might be needed to confirm MetS-induced impairment of MSC-derived EV functional capacity. We likely underestimated the retention of individual EVs, many of which are under the resolution of light microscopy, and counted some clusters. While our data suggest that intra-renal delivery of MetS-EVs is not effective to preserve the stenotic-kidney, future studies are needed to confirm the lack of beneficial effects over longer periods of time. In addition, MSC-derived EVs have a complex cargo that includes not only microRNAs, but also genes and proteins which can also modulate angiogenesis and function in target organs (Aghajani Nargesi et al., 2017). Therefore, MetS-induced changes in genes and proteins packed in MSC-derived EVs might have also contributed to their dysfunction.

5. Conclusion

Taken together, our observations revealed that MetS modifies the microRNA content of EVs isolated from porcine adipose-tissue MSCs, enriching MetS-EVs with microRNAs capable of targeting angiogenic pathways in recipient cells. MetS-EVs failed to induce endothelial cell migration and tube formation in-vitro. Furthermore, intra-renal delivery of MetS-EVs failed to preserve the microvasculature and improve function in pigs with MetS + RAS. Thus, MetS-induced changes in the microRNA content of EVs might exert important post-transcriptional changes in recipient cells, and in turn impair the reparative capacity of EVs.

The current study may therefore contribute to develop approaches to improve the therapeutic efficacy of EVs isolated from adipose tissue-derived MSCs for patients with MetS.

Supplementary Material

Refer to Web version on PubMed Central for supplementary material.

Acknowledgments

Funding

This study was partly supported by NIH grant numbers DK120292, DK104273, DK102325, DK122137, and DK106427.

Declaration of Competing Interest

The authors declare the following financial interests/personal relationships which may be considered as potential competing interests: Dr. Lerman receives grant funding from Novo Nordisk, and is an advisor to Weijian Technologies and AstraZeneca.

References

Aghajani Nargesi A, Lerman LO, Eirin A, 2017. Mesenchymal stem cell-derived extracellular vesicles for kidney repair: current status and looming challenges. Stem Cell Res. Ther 8, 273. [PubMed: 29202871]

Alberti KG, Zimmet P, Shaw J, 2006. Metabolic syndrome–a new world-wide definition. A Consensus Statement from the International Diabetes Federation. Diabet. Med 23, 469–480. [PubMed: 16681555]

Calle A, Barrajon-Masa C, Gomez-Fidalgo E, Martin-Lluch M, Cruz-Vigo P, Sanchez-Sanchez R, Ramirez MA, 2018. Iberian pig mesenchymal stem/stromal cells from dermal skin, abdominal and subcutaneous adipose tissues, and peripheral blood: in vitro characterization and migratory properties in inflammation. Stem Cell Res. Ther 9, 178. [PubMed: 29973295]

Cameron AJ, Shaw JE, Zimmet PZ, 2004. The metabolic syndrome: prevalence in worldwide populations. Endocrinol. Metab. Clin. North Am 33, 351–375. [PubMed: 15158523]

Chade AR, 2011. Renovascular disease, microcirculation, and the progression of renal injury: role of angiogenesis. Am. J. Physiol. Regul. Integr. Comp. Physiol 300, R783–R790. [PubMed: 21307362]

Chade AR, 2013. Renal vascular structure and rarefaction. Compr Physiol. 3, 817–831. [PubMed: 23720331]

Chade AR, Rodriguez-Porcel M, Herrmann J, Zhu X, Grande JP, Napoli C, Lerman A, Lerman LO, 2004. Antioxidant Intervention blunts renal injury in experimental renovascular disease. J. Am. Soc. Nephrol 15, 958–966. [PubMed: 15034098]

Chade AR, Zhu X, Lavi R, Krier JD, Pislaru S, Simari RD, Napoli C, Lerman A, Lerman LO, 2009. Endothelial progenitor cells restore renal function in chronic experimental renovascular disease. Circulation 119, 547–557. [PubMed: 19153272]

Chen Z, Herrmann SM, Zhu X, Jordan KL, Gloviczki ML, Lerman A, Textor SC, Lerman LO, 2014. Preserved function of late-outgrowth endothelial cells in medically treated hypertensive patients under well-controlled conditions. Hypertension 64, 808–814. [PubMed: 25047576]

Chen J, Muntner P, Hamm LL, Jones DW, Batuman V, Fonseca V, Whelton PK, He J, 2004. The metabolic syndrome and chronic kidney disease in U.S. adults. Ann. Intern. Med 140, 167–174. [PubMed: 14757614]

Choi JH, Kim KL, Huh W, Kim B, Byun J, Suh W, Sung J, Jeon ES, Oh HY, Kim DK, 2004. Decreased number and impaired angiogenic function of endothelial progenitor cells in patients with chronic renal failure. Arterioscler. Thromb. Vase. Biol 24, 1246–1252.

Cox J, Hein MY, Luber CA, Paron I, Nagaraj N, Mann M, 2014. Accurate proteome-wide label-free quantification by delayed normalization and maximal peptide ratio extraction, termed MaxLFQ. Mol. Cell. Proteomics 13, 2513–2526. [PubMed: 24942700]

Dudakovic A, Camilleri E, Riester SM, Lewallen EA, Kvasha S, Chen X, Radel DJ, Anderson JM, Nair AA, Evans JM, Kryeh AJ, Smith J, Deyle DR, Stein JL, Stein GS, Im HJ, Cool SM, Westendorf JJ, Kakar S, Dietz AB, van Wijnen AJ, 2014. High-resolution molecular validation of self-renewal and spontaneous differentiation in clinical-grade adipose-tissue derived human mesenchymal stem cells. J. Cell. Biochem 115, 1816–1828. [PubMed: 24905804]

Ebrahimi B, Eirin A, Li Z, Zhu XY, Zhang X, Lerman A, Textor SC, Lerman LO, 2013. Mesenchymal stem cells improve medullary inflammation and fibrosis after revascularization of swine atherosclerotic renal artery stenosis. PLoS ONE 8, e67474. [PubMed: 23844014]

Eirin A, Zhu XY, Urbieta-Caceres VH, Grande JP, Lerman A, Textor SC, Lerman LO, 2011. Persistent kidney dysfunction in swine renal artery stenosis correlates with outer cortical microvascular remodeling. Am. J. Physiol. Renal Physiol 300, F1394–F1401. [PubMed: 21367913]

Eirin A, Zhu XY, Krier JD, Tang H, Jordan KL, Grande JP, Lerman A, Textor SC, Lerman LO, 2012. Adipose tissue-derived mesenchymal stem cells improve revascularization outcomes to restore renal function in swine atherosclerotic renal artery stenosis. Stem Cells. 30, 1030–1041. [PubMed: 22290832]

Eirin A, Li Z, Zhang X, Krier JD, Woollard JR, Zhu XY, Tang H, Herrmann SM, Lerman A, Textor SC, Lerman LO, 2012. A mitochondrial permeability transition pore inhibitor improves renal outcomes after revascularization in experimental atherosclerotic renal artery stenosis. Hypertension 60, 1242–1249. [PubMed: 23045468]

Eirin A, Ebrahimi B, Zhang X, Zhu XY, Tang H, Crane JA, Lerman A, Textor SC, Lerman LO, 2012. Changes in glomerular filtration rate after renal revascularization correlate with microvascular hemodynamics and inflammation in Swine renal artery stenosis. Circ. Cardiovasc. Interv 5, 720–728. [PubMed: 23048054]

Eirin A, Riester SM, Zhu XY, Tang H, Evans JM, O'Brien D, van Wijnen AJ, Lerman LO, 2014. MicroRNA and mRNA cargo of extracellular vesicles from porcine adipose tissue-derived mesenchymal stem cells. Gene 551, 55–64. [PubMed: 25158130]

Eirin A, Williams BJ, Ebrahimi B, Zhang X, Crane JA, Lerman A, Textor SC, Lerman LO, 2014. Mitochondrial targeted peptides attenuate residual myocardial damage after reversal of experimental renovascular hypertension. J. Hypertens 32, 154–165. [PubMed: 24048008]

Eirin A, Zhang X, Zhu XY, Tang H, Jordan KL, Grande JP, Dietz AB, Lerman A , Textor SC, Lerman LO, 2014. Renal vein cytokine release as an index of renal parenchymal inflammation in chronic experimental renal artery stenosis. Nephrol. Dial. Transplant 29, 274–282. [PubMed: 24097799]

Eirin A, Zhu XY, Puranik AS, Woollard JR, Tang H, Dasari S, Lerman A, van Wijnen AJ, Lerman LO, 2016. Comparative proteomic analysis of extracellular vesicles isolated from porcine adipose tissue-derived mesenchymal stem/stromal cells. Sci. Rep 6, 36120. [PubMed: 27786293]

Eirin A, Zhu XY, Puranik AS, Woollard JR, Tang H, Dasari S, Lerman A, van Wijnen AJ, Lerman LO, 2017. Integrated transcriptomic and proteomic analysis of the molecular cargo of extracellular vesicles derived from porcine adipose tissue-derived mesenchymal stem cells. PLoS ONE 12, e0174303. [PubMed: 28333993]

Eirin A, Zhu XY, Puranik AS, Tang H, McGurren KA, van Wijnen AJ, Lerman A, Lerman LO, 2017. Mesenchymal stem cell-derived extracellular vesicles attenuate kidney inflammation. Kidney Int. 92, 114–124. [PubMed: 28242034]

Eirin A, Zhu XY, Jonnada S, Lerman A, van Wijnen AJ, Lerman LO, 2018. Mesenchymal stem cell-derived extracellular vesicles improve the renal microvasculature in metabolic renovascular disease in swine. Cell Transplant. 27, 1080–1095. [PubMed: 29954220]

Ferguson CM, Eirin A, Michalak GJ, Hedayat AF, Abumoawad A, Saad A, Zhu X, Textor SC, McCollough CH, Lerman LO, 2018. Intrarenal fat deposition does not interfere with the measurement of single-kidney perfusion in obese swine using multi-detector computed tomography. J. Cardiovasc. Comput. Tomogr 12, 149–152. [PubMed: 29339048]

Ferguson CM, Eirin A, Michalak GJ, Hedayat AF, Abumoawad AM, Saad A, Zhu X , Textor SC, McCollough CH, Lerman LO, 2019. Renal adiposity does not preclude quantitative assessment of renal function using dual-energy multidetector CT in mildly obese human subjects. Acad. Radiol.

Hansen KJ, Edwards MS, Craven TE, Cherr GS, Jackson SA, Appel RG, Burke GL, Dean RH, 2002. Prevalence of renovascular disease in the elderly: a population-based study. J. Vase. Surg 36, 443–451.

Hogan MC, Bakeberg JL, Gainullin VG, Irazabal MV, Harmon AJ, Lieske JC, Charlesworth MC, Johnson KL, Madden BJ, Zenka RM, McCormick DJ, Sundsbak JL, Heyer CM, Torres VE, Harris PC, Ward CJ, 2015. Identification of biomarkers for PKD1 using urinary exosomes. J. Am. Soc. Nephrol 26, 1661–1670. [PubMed: 25475747]

Huang R, Qin C, Wang J, Hu Y, Zheng G, Qiu G, Ge M, Tao H, Shu Q, Xu J, 2019. Differential effects of extracellular vesicles from aging and young mesenchymal stem cells in acute lung injury. Aging (Albany NY). 11, 7996–8014. [PubMed: 31575829]

Kalari KR, Nair AA, Bhavsar JD, O'Brien DR, Davila JI, Bockol MA, Nie J, Tang X, Baheti S, Doughty JB, Middha S, Sicotte H, Thompson AE, Asmann YW, Kocher JP, 2014. MAP-RSeq: Mayo Analysis Pipeline for RNA sequencing. BMC Bioinf. 15, 224.

Kim D, Pertea G, Trapnell C, Pimentel H, Kelley R, Salzberg SL, 2013. TopHat2: accurate alignment of transcriptomes in the presence of insertions, deletions and gene fusions. Genome Biol. 14, R36. [PubMed: 23618408]

Kim KI, van de Wiel MA, 2008. Effects of dependence in high-dimensional multiple testing problems. BMC Bioinf. 9, 114.

Krier JD, Ritman EL, Bajzer Z, Romero JC, Lerman A, Lerman LO, 2001. Noninvasive measurement of concurrent single-kidney perfusion, glomerular filtration, and tubular function. Am. J. Physiol. Renal Physiol 281, F630–F638. [PubMed: 11553509]

Lerman LO, Schwartz RS, Grande JP, Sheedy PF, Romero JC, 1999. Noninvasive evaluation of a novel swine model of renal artery stenosis. J. Am. Soc. Nephrol 10, 1455–1465. [PubMed: 10405201]

Lerman L, Textor SC, 2001. Pathophysiology of ischemic nephropathy. Urol. Clin. North Am 28 (793–803), ix.

Liao Y, Smyth GK, Shi W, 2014. featureCounts: an efficient general purpose program for assigning sequence reads to genomic features. Bioinformatics 30, 923–930. [PubMed: 24227677]

Meng Y, Eirin A, Zhu XY, Tang H, Chanana P, Lerman A, Van Wijnen AJ, Lerman LO, 2018. The metabolic syndrome alters the miRNA signature of porcine adipose tissue-derived mesenchymal stem cells. Cytometry A. 93, 93–103. [PubMed: 28678424]

Miller JE, Monsanto SP, Ahn SH, Khalaj K, Fazleabas AT, Young SL, Lessey BA, Koti M, Tayade C, 2017. Interleukin-33 modulates inflammation in endometriosis. Sci. Rep 7, 17903. [PubMed: 29263351]

Mol EA, Goumans MJ, Doevendans PA, Sluijter JPG, Vader P, 2017. Higher functionality of extracellular vesicles isolated using size-exclusion chromatography compared to ultracentrifugation. Nanomedicine 13, 2061–2065. [PubMed: 28365418]

Moran-Jones K, Brown LM, Samimi G, 2015. INC280, an orally available small molecule inhibitor of c-MET, reduces migration and adhesion in ovarian cancer cell models. Sci. Rep 5, 11749. [PubMed: 26138303]

Nargesi AA, Lerman LO, Eirin A, 2017. Mesenchymal stem cell-derived extracellular vesicles for renal repair. Curr. Gene Ther 17, 29–42. [PubMed: 28403795]

Pawar AS, Zhu XY, Eirin A, Tang H, Jordan KL, Woollard JR, Lerman A, Lerman LO, 2015. Adipose tissue remodeling in a novel domestic porcine model of diet-induced obesity. Obesity (Silver Spring) 23, 399–407. [PubMed: 25627626]

Pawar AS, Eirin A, Krier JD, Woollard JR, Zhu XY, Lerman A, van Wijnen AJ, Lerman LO, 2019. Alterations in genetic and protein content of swine adipose tissue-derived mesenchymal stem cells in the metabolic syndrome. Stem Cell Res. 37, 101423. [PubMed: 30933719]

Reiner AT, Witwer KW, van Balkom BWM, de Beer J, Brodie C, Corteling RL, Gabrielsson S, Gimona M, Ibrahim AG, de Kleijn D, Lai CP, Lotvall J, Del Portillo HA, Reischl IG, Riazifar M, Salomon C, Tahara H, Toh WS, Wauben MHM, Yang VK, Yang Y, Yeo RWY, Yin H, Giebel B, Rohde E, Lim SK, 2017. Concise review: developing best-practice models for the therapeutic use of extracellular vesicles. Stem Cells Transl. Med 6, 1730–1739. [PubMed: 28714557]

Roberts CK, Hevener AL, Barnard RJ, 2013. Metabolic syndrome and insulin resistance: underlying causes and modification by exercise training. Compr Physiol. 3, 1–58. [PubMed: 23720280]

Robinson MD, McCarthy DJ, Smyth GK, 2010. edgeR: a Bioconductor package for differential expression analysis of digital gene expression data. Bioinformatics 26, 139–140. [PubMed: 19910308]

Saad A, Dietz AB, Herrmann SMS, Hickson LJ, Glockner JF, McKusick MA, Misra S, Bjarnason H, Armstrong AS, Gastineau DA, Lerman LO, Textor SC, 2017. Autologous mesenchymal stem cells increase cortical perfusion in renovascular disease. J. Am. Soc. Nephrol 28, 2777–2785. [PubMed: 28461553]

Schneider CA, Rasband WS, Eliceiri KW, 2012. NIH Image to ImageJ: 25 years of image analysis. Nat. Methods 9, 671–675. [PubMed: 22930834]

Siegel G, Kluba T, Hermanutz-Klein U, Bieback K, Northoff H, Schafer R, 2013. Phenotype, donor age and gender affect function of human bone marrow-derived mesenchymal stromal cells. BMC Med. 11, 146. [PubMed: 23758701]

Sun Z, Evans J, Bhagwate A, Middha S, Bockol M, Yan H, Kocher JP, 2014. CAP-miRSeq: a comprehensive analysis pipeline for microRNA sequencing data. BMC Genomics 15, 423. [PubMed: 24894665]

Togliatto G, Dentelli P, Gili M, Gallo S, Deregibus C, Biglieri E, Iavello A, Santini E, Rossi C, Solini A, Camussi G, Brizzi MF, 2016. Obesity reduces the pro-angiogenic potential of adipose tissue stem cell-derived extracellular vesicles (EVs) by impairing miR-126 content: impact on clinical applications. Int. J. Obes. (Lond.) 40, 102–111. [PubMed: 26122028]

Troyanovsky B, Levchenko T, Mansson G, Matvijenko 0, Holmgren L, 2001. Angiomotin: an angiostatin binding protein that regulates endothelial cell migration and tube formation. J Cell Biol. 152, 1247–1254. [PubMed: 11257124]

Wang J, Wang J, Dai J, Jung Y, Wei CL, Wang Y, Havens AM, Hogg PJ, Keller ET, Pienta KJ, Nor JE, Wang CY, Taichman RS, 2007. A glycolytic mechanism regulating an angiogenic switch in prostate cancer. Cancer Res. 67, 149–159. [PubMed: 17210694]

Wajih N, Sane DC, 2003. Angiostatin selectively inhibits signaling by hepatocyte growth factor in endothelial and smooth muscle cells. Blood 101, 1857–1863. [PubMed: 12406896]

Zhu XY, Chade AR, Rodriguez-Pore el M, Bentley MD, Ritman EL, Lerman A, Lerman LO, 2004. Cortical microvascular remodeling in the stenotic kidney: role of increased oxidative stress. Arterioscler Throm. Vase. Biol 24, 1854–1859.

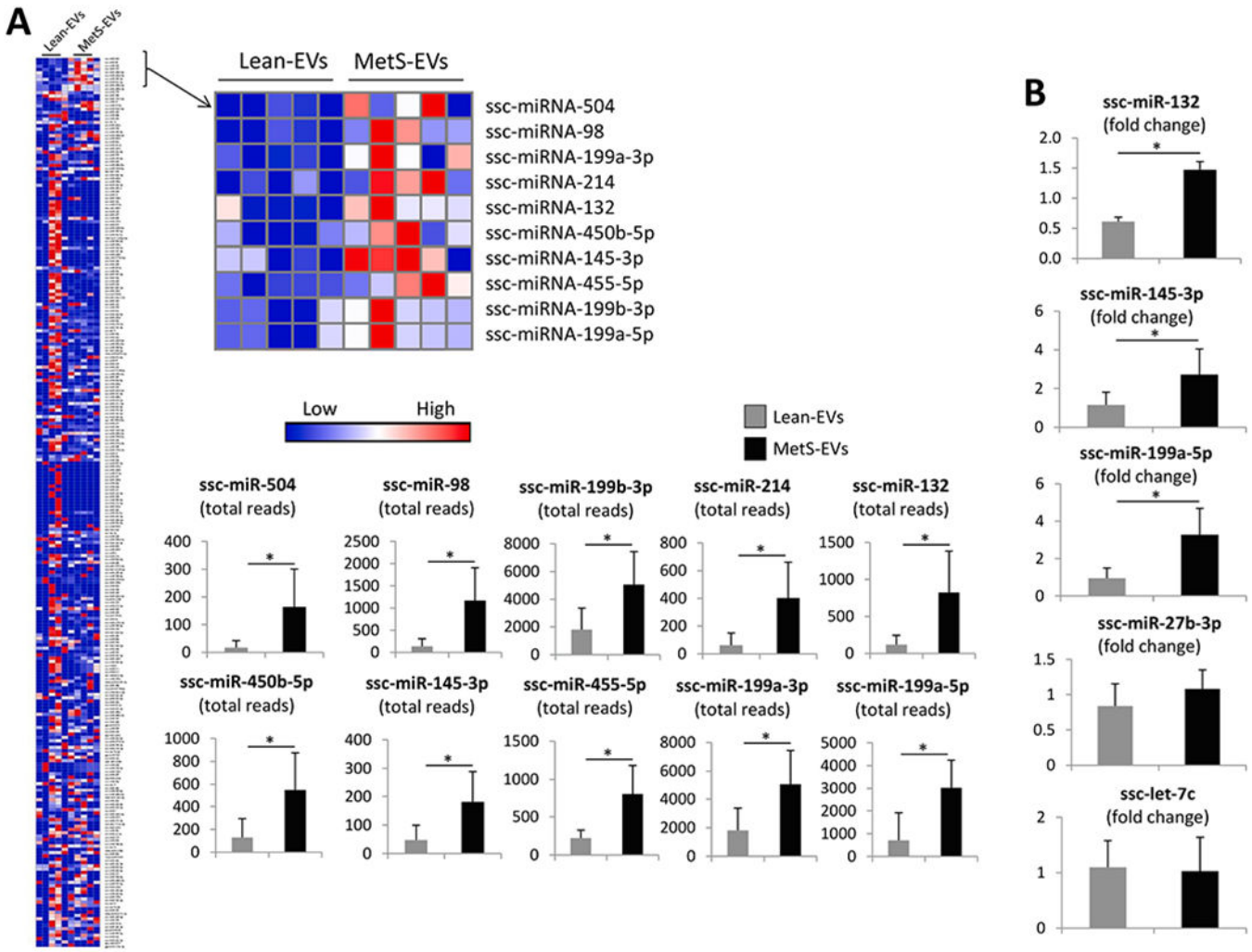

Fig. 1. MetS alters the microRNA cargo of EVs.

A. Representative heat map and quantification of the relative expression of 10 microRNAs upregulated in MetS-EVs compared to Lean-EVs. B: Quantitative polymerase chain reaction of miR-132, miR-145–3p, miR-199a-5p, miR-27b, and let-7c followed the same pattern as microRNA sequencing. *$p < 0.05$.

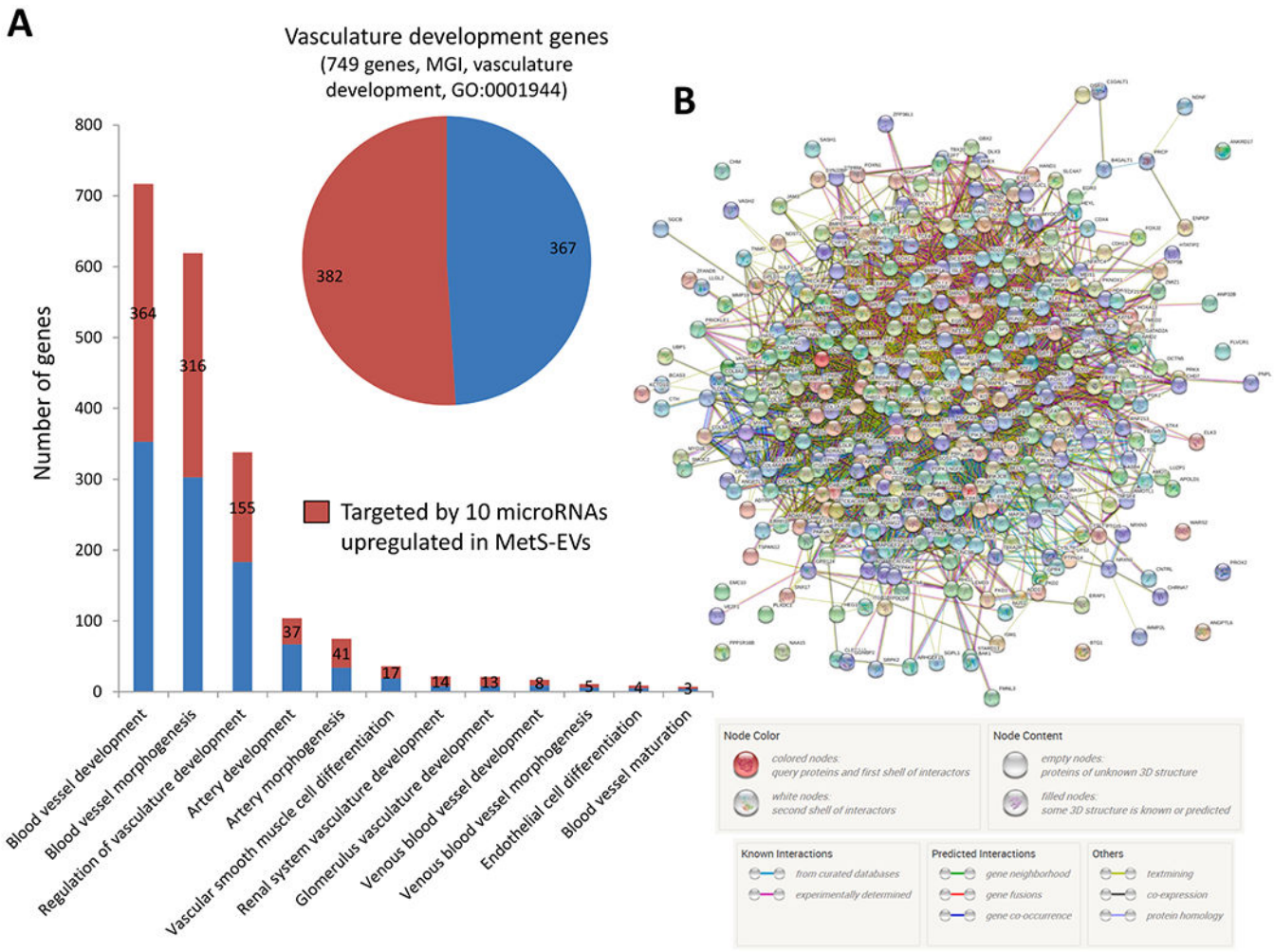

Fig. 2. microRNAs upregulated in MetS-EVs target pro-angiogenic genes.

A. Target gene prediction analysis shows that microRNAs enriched in MetS-EVs are capable of targeting 382 out of 749 genes associated with vasculature development (MGI, vasculature development, GO:0001944). B. Interactions among pro-angiogenic genes targeted by microRNAs upregulated in MetS-EVs derived from STRING. Nodes represent genes targeted by microRNAs upregulated in MetS-EVs, and color lines their interactions according to the functional association networks from the STRING database.

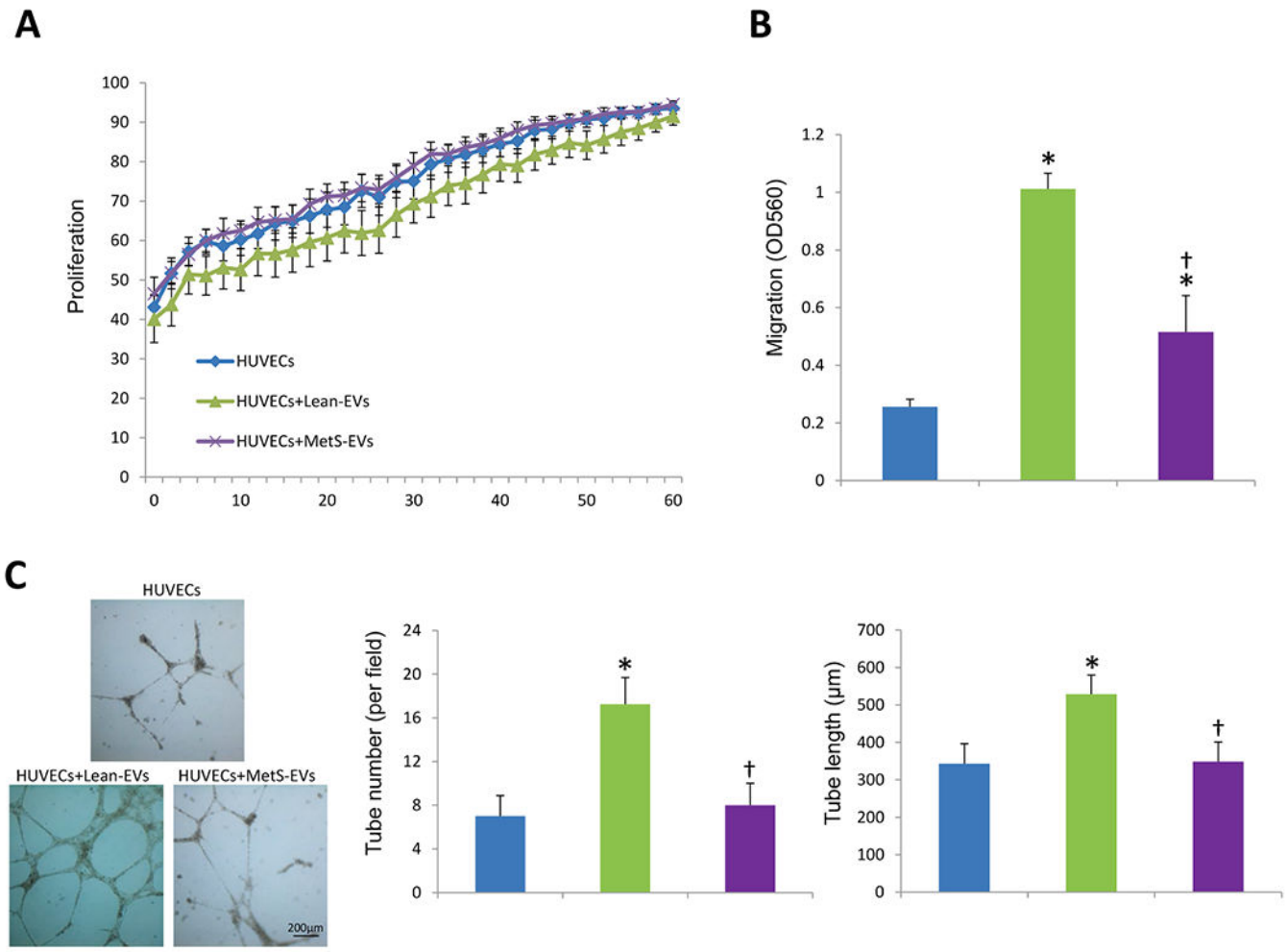

Fig. 3. ***MetS-EVs failed to induce endothelial cell tube formation*** **in vitro.**

A: Human umbilical endothelial cells (HUVEC) proliferation was similar among the groups. B: Migration increased in cells treated with EVs, but the increase was greater in Lean-EVs compared to MetS-EVs. C: The number and length of tubular-like structures formed in matrigel were higher in HUVECs + Lean-EVs compared to untreated HUVECs and HUVECs + MetS-EVs. *p < 0.05 vs. HUVECs, †p < 0.05 vs. HUVECs + Lean-EVs.

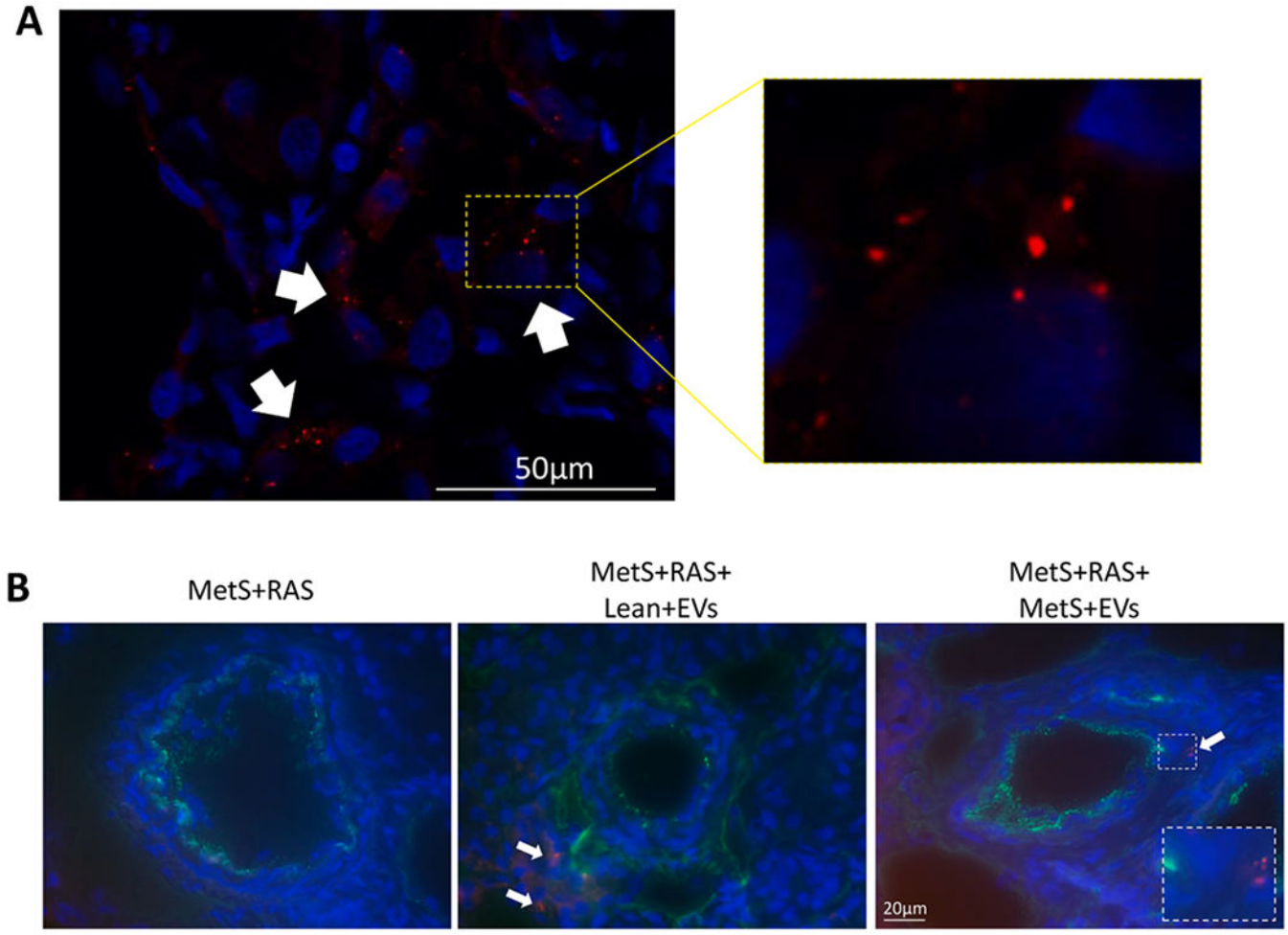

Fig. 4. EVs were retained in the stenotic kidney.

A: EV clusters (red) were detected in the tubulo-interstitium of porcine stenotic-kidneys 4 weeks after intra-renal delivery (arrows). B: Immunofluorescence co-staining with the endothelial cell marker CD 31 (both green) shows EV clusters in the proximity of small vessels (box). (For interpretation of the references to color in this figure legend, the reader is referred to the web version of this article.)

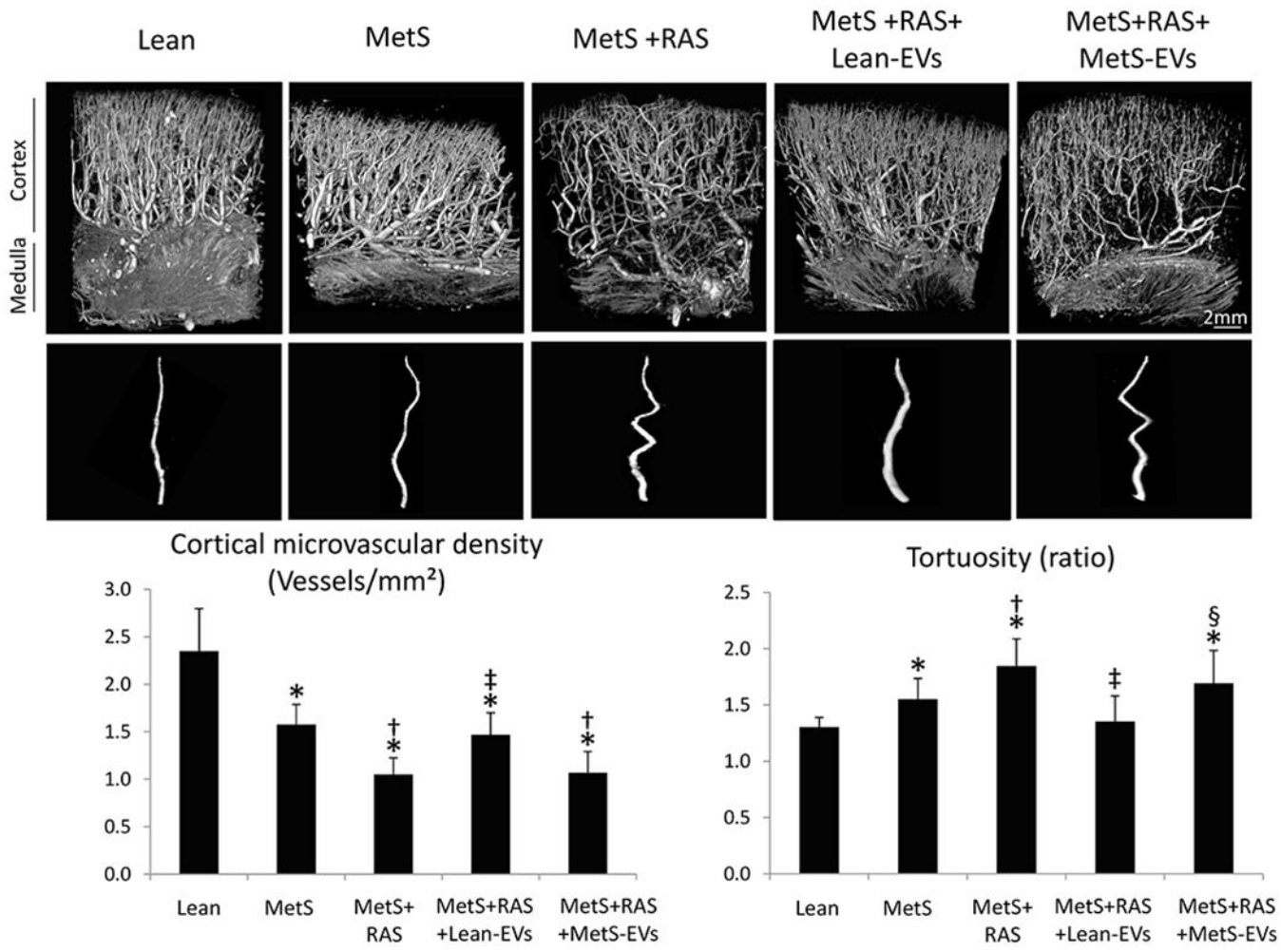

Fig. 5. MetS-EVs failed to improve renal microvascular density.

A: Representative three-dimensional microcomputed tomography images of the kidney. B: Quantification of spatial density of cortical microvessels and vessel tortuosity, *p < 0.05 vs. Lean, †p < 0.05 vs. MetS, ‡p < 0.05 vs. MetS + RAS, §p < 0.05 vs. MetS + RAS + Lean-EVs.

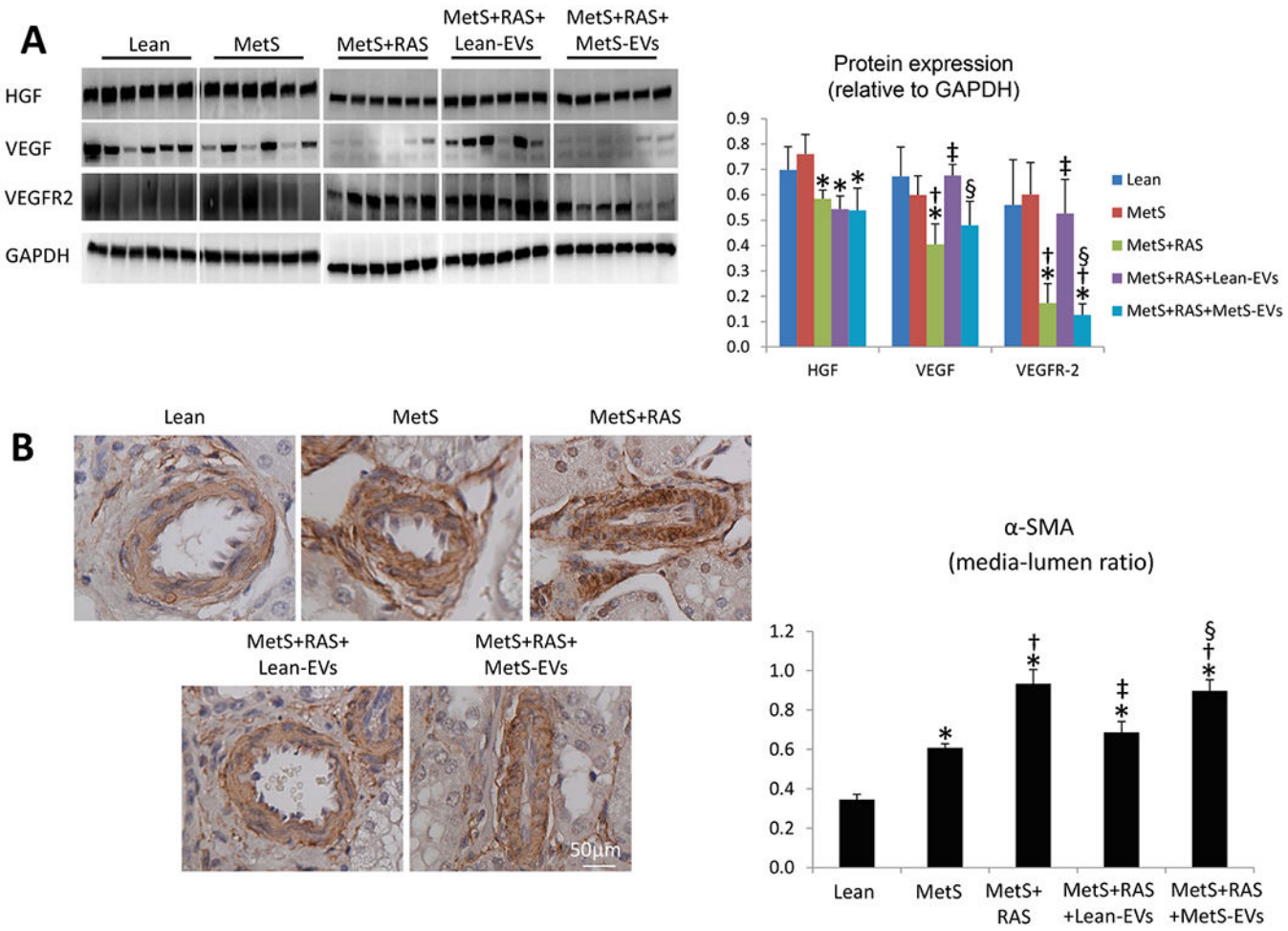

Fig. 6. MetS-EVs did not improve microvascular remodeling.

A: Renal protein expression of hepatocyte growth factor (HGF), vascular endothelial growth factor (VEGF), and VEGF receptor (VEGFR) — 2. B: Representative kidney α-smooth muscle actin (SMA) staining and quantification of renal vessel wall-to-lumen ratio. *$p < 0.05$ vs. Lean, †$p < 0.05$ vs. MetS, ‡$p < 0.05$ vs. MetS + RAS, §$p < 0.05$ vs. MetS + RAS + Lean-EVs.

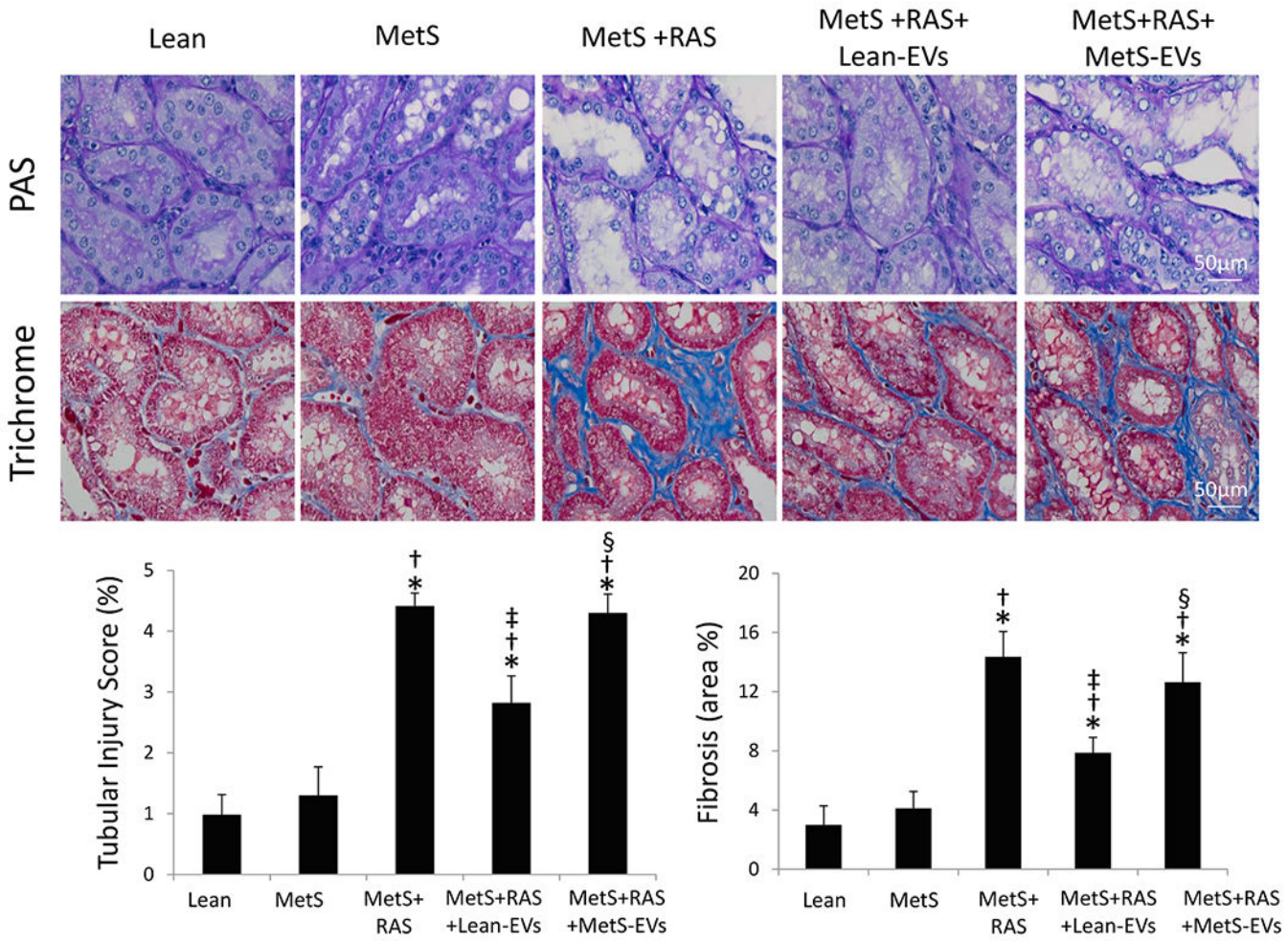

Fig. 7. MetS-EVs did not attenuate renal fibrosis.

Representative kidney periodic acid-Schiff (PAS) and trichrome staining (40X), and quantifications of tubular injury and tubulo-interstitial fibrosis. *p < 0.05 vs. Lean, †p < 0.05 vs. MetS, ‡p < 0.05 vs. MetS + RAS, §p < 0.05 vs. MetS + RAS + Lean-EVs.

Table 1

Systemic characteristics and single-kidney function in study groups at 16 weeks.

	Lean	MetS	MetS + RAS	MetS + RAS + LeanEVs	MetS + RAS + MetS-EVs
Body weight (Kg)	70.9 ± 9.2	96.9 ± 4.3 *	92.0 ± 5.3 *	91.6 ± 8.6 *	90.9 ± 8.2 *
MAP (mmHg)	92.0 ± 5.3	123.7 ± 9.0 *	130.5 ± 16.3 *	118.5 ± 12.3 *	126.3 ± 6.4 *
Degree of stenosis (%)	0	0	64.3 ± 17.9 *†	65.7 ± 7.9 *†	66.4 ± 6.3 *†
Total cholesterol (mg/dl)	87.0 (78.1–90.0)	342.9 (318.3–481.0) *	345.1 (325.5–406.2) *	345.2 (314.2–413.2) *	316.5 (312.4–400.2) *
HDL cholesterol (mg/dl)	49.1 (45.0–50.2)	123.0 (110.1–154.2) *	132.1 (99.0–136.1) *	127.0 (98.1–132.1) *	125.1 (102.0–129.1) *
LDL cholesterol (mg/dl)	33.9 ± 6.1	361.2 ± 129.3 *	345.5 ± 81.7 *	357.4 ± 43.6 *	344.8 ± 39.8 *
Triglycerides (mg/dl)	7.6 (6.0–9.1)	14.3 (13.1–22.5) *	14.21 (13.1–15.1) *	16.3 (13.5–17.3) *	15.5 (12.4–21.1) *
Fasting glucose (mg/dl)	125.5 ± 15.5	118.6 ± 18.0	114.8 ± 13.3	113.9 ± 16.5	118.4 ± 17.3
Fasting insulin (μU/ml)	0.4 (0.4–0.5)	0.8 (0.7–0.8) *	0.8 (0.7–0.8) *	0.8 (0.7–0.8) *	0.7 (0.7–0.8) *
HOMA-IR score	0.6 (0.5–0.7)	1.9 (1.8–1.9) *	1.8 (1.7–1.9) *	1.7 (1.7–1.8) *	1.8 (1.5–1.9) *
Renal volume (ml)	134.4 ± 15.6	219.3 ± 19.1 *	180.5 ± 21.8 *†	234.9 ± 49.0 *‡	172.1 ± 28.3 *†‡§
RBF (ml/min)	502.8 ± 70.6	848.0 ± 202.4 *	629.5 ± 72.4 *†	877.2 ± 260.7 *‡	673.9 ± 75.5 *†§
GFR (ml/min)	76.5 ± 10.5	140.4 ± 23.2 *	95.5 ± 12.6 *†	130.3 ± 33.9 *‡	101.0 ± 22.0 *†§

MAP: mean arterial pressure; HDL: high-density lipoprotein; LDL: low-density lipoprotein; HOMA-IR: homeostasis model assessment of insulin resistance; RBF: renal blood flow; GFR: glomerular filtration rate.

*$p < 0.05$ vs. Lean;

†$p < 0.05$ vs. MetS;

‡$p < 0.05$ vs. MetS + RAS;

§$p < 0.05$ vs. MetS + RAS + Lean-EVs.